Progress In Electromagnetics Research C, Vol. 113, 69–82, 2021

A Compact Four-Port High Isolation Hook Shaped ACS Fed MIMO Antenna for Dual Frequency Band Applications

Praveen V. Naidu[1, 2, *], Dhanekula Maheshbabu[1, 2, 5], Akkapanthula Saiharanadh[1, 2, 4], Arvind Kumar[2, 3], Neelima Vummadisetty[2], Lam Sumanji[1], and Khalim A. Meerja[1]

Abstract—In this work, a novel 4 element Multi-Input Multi-Output (MIMO) antenna is reported. The proposed antenna has a size of $50 \times 50 \times 1.6\,\text{mm}^3$ is printed on the FR-4 substrate having dielectric constant $\varepsilon_r = 4.4$ and loss tangent ($\tan\delta = 0.02$). The four antenna elements are positioned in each corner of the PCB board in an orthogonal manner such that they can provide better isolation between antenna elements. The proposed MIMO antenna is designed to operate in frequency bands of 2.25 GHz to 2.4 GHz and 4.7 GHz to 6.3 GHz. The lower band ranges from 2.25 GHz to 2.4 GHz and covers 2.3 GHz WiBro applications while the upper band ranging from 4.7 GHz to 6.3 GHz is useful for HiperLAN and Wi-MAX applications. The proposed antenna acquires return loss less than −10 dB and isolated by more than 16 dB throughout the dual operating bands. The structure exhibits stable gain and radiation patterns. Various diversity performance metrics including envelope correlation coefficient (ECC), diversity gain (DG), and mean effective gain (MEG) are evaluated and are within acceptable limits. Full wave simulation results in terms of impedance and radiation characteristics are presented to evaluate the proposed antenna performance in an installed environment.

1. INTRODUCTION

Recently, the advancement of mobile wireless communication has been evolving swiftly from universal mobile telecommunication system (UMTS), global system of mobile communication (GSM) to wireless local area networks (WLAN), and long-term evolution (LTE), and a higher level is accomplished in terms of data transfer rates as per needs of mobile terminals than ever before. For the high-speed data transmission, mostly used wireless standards are Long-Term Evolution (LTE), Worldwide Interoperability for Microwave Access (WiMAX) IEEE 802.16, and Wireless Local Area Network (WLAN) IEEE 802.11 a/b/g. With multiple antennas, MIMO technology is efficacious in the enhancement of system capacity while offering the guarantee of a high data rate. Due to the advancement in technology and development in portable devices, there is a requirement to cover more than one frequency band in wireless applications. Therefore, more individual antennas are designed to meet this requirement. Hence, a multiband antenna is preferable instead of utilizing an individual antenna for each wireless application. By using various radiating patches such as rhombic slot antenna with a truncated corner [1], two branch strips [2], inverted-F antenna [3], L-shape and E-shape radiating patches [4], and meander line with branch [5], different types of multiband antennas are developed with good return loss characteristics for the different wireless applications. The compactness of the antenna is achieved by considering the suitable feeding technique.

Asymmetric coplanar strip (ACS) and coplanar waveguide (CPW) feeding techniques are widely used for low profile antennas. In [6], a compact ACS-fed multiband antenna with an M-shape patch

Received 27 April 2021, Accepted 5 June 2021, Scheduled 10 June 2021
* Corresponding author: Praveen Vummadisetty Naidu (praveennaidu468@gmail.com).
[1] VRSEC, Vijayawada 520007, India. [2] Department of R&D, NPHSAT Systems Pvt Ltd, Vijayawada 520007, India. [3] University of East London, UK. [4] DRDO, Hyderabad, India. [5] TCS, Hyderabad, India.

loaded with rectangular and L-shaped strips is developed with the dimensions $12.5 \times 18\,\text{mm}^2$ on an FR4 substrate with a thickness of 1.6 mm. It can be seen that meandered mirrored S-shaped strip (0.5λ), mirrored L-shaped radiating branch (0.29λ), and monopole (0.25λ) are responsible for achieving the first, second, third operating bands [7]. For the PCS/WLAN/WiMAX applications, ACS fed tri-band antenna with the area of $516\,\text{mm}^2$ is reported in [8]. An O-shaped antenna with the compact dimensions of $20 \times 12.5 \times 1.6\,\text{mm}^3$ is designed for the dual-band applications, which is excited by ACS fed technique reported in [9]. In [10], an ACS fed meandered shape structured monopole antenna is proposed with wide impedance bandwidth. Dual-band antennas for various wireless applications are designed by using a hexagonal radiating patch [11], two stepped rectangular patches [12], a modified rectangular radiating patch [13], a hexagonal patch loaded with a strip [14], and all are excited by adopting CPW-fed mechanism. From the above discussion, it is clear that the overall size of the antenna is minimized in the case of using the ACS fed technique.

Low channel capacity, low data rate, and high latency are the constraints while the single element is used. On the other hand, MIMO technology is considered to achieve high data rates, low latency, throughput, and high channel capacity. Multiple antennas are used in the MIMO system; therefore, fading effect will be minimized. However, the performance of the MIMO system is degraded by the mutual coupling between antenna elements. To achieve the high isolation between antenna elements, different types of isolation techniques are reported in the literature for-instance transmission lines ($S_{21} > -15\,\text{dB}$) [15], diagonally opposite position ($S_{21} > -12\,\text{dB}$) [16], orthogonality between elements ($S_{21} > -12\,\text{dB}$) [17], ($S_{21} < -14\,\text{dB}$) [18], ($S_{21} = -18\,\text{dB}$) [19], placing in opposite manner ($S_{21} > -19\,\text{dB}$) [20], transmission lines and slots ($S_{21} > -25\,\text{dB}$) [21], a shorting strip and stub ($S_{21} > -27\,\text{dB}$) [22], a stepped slot ended with an ellipse ($S_{21} < -18\,\text{dB}$) [23], a parasitic element ($S_{21} < -15\,\text{dB}$) [24], a decoupling structure ($S_{21} < -24\,\text{dB}$) [25], separation between elements ($S_{21} < -20\,\text{dB}$) [26], vertical position ($S_{21} = -16.5\,\text{dB}$) [27], meandering line and decoupling structure ($S_{21} < -25\,\text{dB}$) [28], ($S_{21} < -26.57\,\text{dB}$) [29], symmetric slot lines and reversed alignment of radiators ($S_{21} > -15\,\text{dB}$) [30], defected ground plane and neutralization lines ($S_{21} < -17\,\text{dB}$) [31], microstrip resonator ($S_{21} > -35\,\text{dB}$) [32], a T-shape isolator ($S_{21} > -12.4\,\text{dB}$) [33], a decoupling structure with branches and slots ($S_{21} < -15\,\text{dB}$) [34], and parallel arrangement ($S_{21} > -18\,\text{dB}$) [35].

Table 1 gives a summary of published literature. The proposed four-port ACS fed hook shaped MIMO antenna is compared with prior art concerning antenna profile, area, number of radiating elements, number of operating bands, isolation between radiating elements, and different diversity parameters. With this comparison, it can be seen that the proposed MIMO antenna operates in dual bands with a peak gain of 4 dB for wireless applications with the minimum mutual coupling of $-16\,\text{dB}$ and a good channel capacity loss less than 0.2 bps/Hz.

In this paper, we propose a four-element ACS fed hook shaped MIMO antenna in which reduction of mutual coupling between antenna elements is achieved by the orthogonal placement of antenna elements. The performance of the proposed ACS fed hook shaped MIMO antenna is investigated in terms of diversity parameters.

2. DESIGN OF ANTENNA

2.1. Unit Element

The fundamental element of the proposed Hook [36] shaped ACS fed MIMO antenna structure is illustrated in Fig. 1. An ACS-fed antenna is a very popular choice for designing small antennae due to its ability to produce wideband within a smaller area than a conventional microstrip antenna. The proposed unit element was printed on a highly available FR4 epoxy substrate ($\varepsilon_r = 4.4$ & $\tan\delta = 0.02$) having dimensions of $24 \times 10 \times 1.6\,\text{mm}^3$. To obtain desired frequency in design, the length of the rectangle-shaped radiating strip and open half hexagon are chosen approximately equal to half of the wavelength ($\lambda/2$). The frequency band between 5 and 6 GHz is achieved by attaching the single radiating patch to the ACS feedline. To get another frequency band at a lower frequency, a Hook shape is added to the radiating patch and ACS feedline.

The design parameters of the proposed antenna shown in Fig. 1 are mentioned below (all values are in mm). $L = 24$, $L1 = 7.8$, $L2 = 4.3$, $L3 = 3.7$, $L4 = 3.4$, $L5 = 4$, $W = 10$, $W1 = 4.4$, $W2 = 2.2$, $W3 = 2$, $W4 = 4.2$, $W5 = 3$, $W6 = 4$, $g1 = 1.9$, $g2 = 1.6$, $g3 = 1.6$, $g4 = 1.3$, $G = 0.5$.

Table 1.

S. No.	Ref. [no]	Size (mm × mm)	Area (mm × mm)	No. of Ports	Operating frequency (GHz)	Avg Gain (dB/dBi)	Minimum isolation	ECC	CCL
1.	[1]	40 × 40	1600	Single	3.15–3.7 /5.05–5.97	∼ 3 dBi	-	-	-
2.	[2]	30 × 35	1050	Single	2.28–2.77 /5–6.3	-	-	-	-
3.	[3]	37 × 40	1480	single	2.28–4.16 /4.97–7.19	∼ 2.1 dBi	-	-	-
4.	[4]	33 × 30	660	Single	2.2–2.5 /4.5–5.2	-	-	-	-
5.	[5]	40 × 30	1200	single	2.39–2.5 /5–6.1	∼ 2 dBi	-	-	-
6.	[15]	55 × 64	3520	2	2.35/3.5	2.76 dB	−15	< 0.001	-
7.	[16]	120 × 100	12,000	2	2.2–2.7 /3.3–4.02	3.95 dBi	> 12	< 0.0056	
8.	[17]	60 × 100	6000	2	2.45/5.5	−0.825 dBi	−16	< 0.1	-
9.	[18]	58 × 55	3132	2	2.1/2.5/3.5 /5.2/5.8	2.5 dB	< −14	< 0.02	-
10.	[20]	89 × 86	7654	4	2.52/5.73	3 dBi	> 19	< 0.05	
11.	[21]	30 × 65	1950	2	2.4/5.5	4.34 dB	−25	< 0.1	-
12.	[22]	50 × 80	4000	2	2.4/5.8	4.12 dB	−20	0.01	-
13.	[23]	50 × 50	2500	2	2.4/3.5/5.5	3.3 dB	−18	< 0.03	-
14.	[24]	100 × 130	13000	2	2.44/5.5	2.1 dB	−22	0.12	-
15	[25]	60 × 60	3600	4	2.46/3.5	3 dBi	< 26	< 0.007	
16.	[26]	75 × 66	4950	2	2.4/5.5	3.34 dB	−22	< 0.25	-
17.	[27]	150 × 75	11,250	4	3.5/5	4.85 dBi	> 16.5	0.01	
18.	[28]	60 × 60	3600	2	2.44/5.48	-	−25	< 0.08	-
19.	[30]	84 × 26	2184	4	3.5/5.5/7	-	−28	-	-
20.	[19]	60 × 60	3600	4	2.5/5.2	3.82 dB	−18	< 0.004	-
21.	[29]	100 × 55	5500	2	2.45/5.25	-	−25	0.001	-
22.	[31]	90 × 40	3600	2	3.3	1.2 dBi	−17	0.005	0.4
23.	[32]	54.7 × 37.5	2051.25	4	5.2	-	−44	-	-
24.	[33]	65.3 × 65.3	4264.09	2	2.4/3.5	2.6 dB	−12.4	< 0.01	-
25.	[34]	60 × 130	7800	4	2.45/5.2/5.8	3 dB	< −15	< 0.25	-
26.	**proposed**	**50 × 50**	**2500**	**4**	**2.25–2.41 /4.7–6.25**	**4 dB**	**> −16**	**0.025**	**0.2**

The evolution of the fundamental element involves two steps, and the basic monopole antenna named antenna #1 and the proposed antenna named antenna #2 are shown in Fig. 2. The frequency band between 5 and 6 GHz is achieved by attaching the single radiating patch (antenna #1) to the ACS feedline shown in Fig. 2(a). In order to get another frequency band at a lower frequency, a Hook shape (proposed antenna) is added to the radiating patch and ACS feedline as illustrated in Fig. 2(b). The impedance matching characteristics of the evolution stages of the fundamental element are illustrated in Fig. 3.

Surface current distribution characteristics of the ACS fed hook shaped dual-band antenna at 2.4 GHz and 5.5 GHz is plotted in Fig. 4. It is clear that the basic monopole antenna (antenna #1) is responsible for higher operating band, and the Hook shape patch (antenna #2) is responsible for lower operating band.

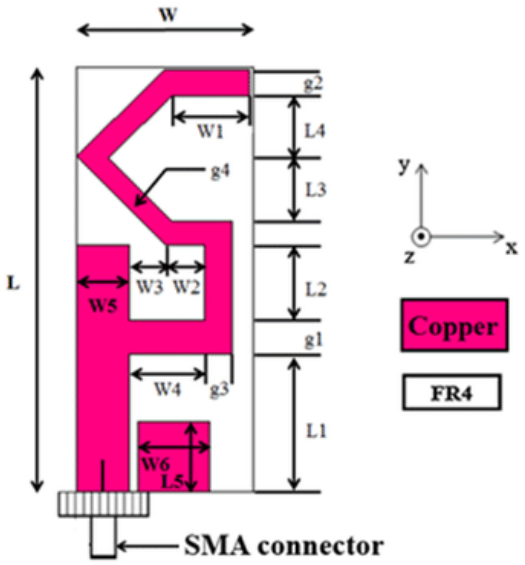

Figure 1. Geometry of the single element.

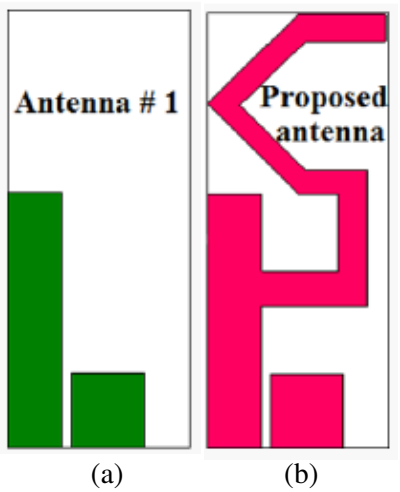

Figure 2. Evolution of fundamental element.

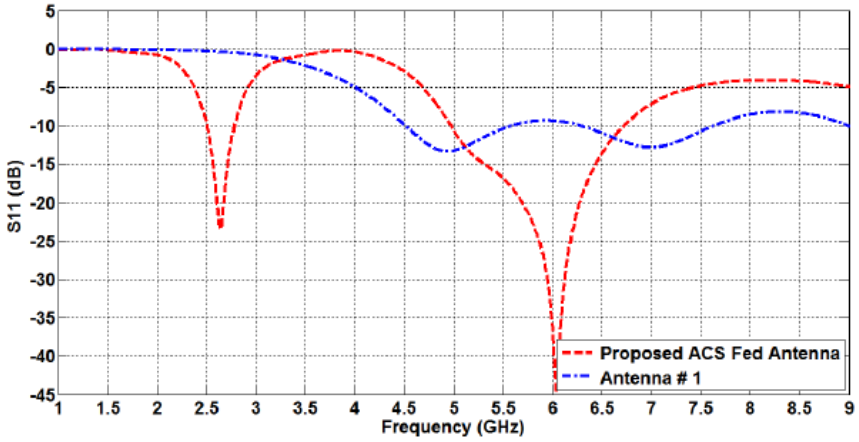

Figure 3. Impedance matching characteristics during evolution of unit element.

2.2. MIMO Antenna

While the MIMO antenna is designed, the mutual coupling between the antenna elements is the main constraint because in a MIMO system the distance between the antenna elements should not be less than half lambda of the operating frequency (i.e., lower operating frequency is considerable). As shown in Fig. 5(a), at first a two-port system is considered where the elements are placed in parallel and mirror positions with dimensions $25 \times 50 \times 1.6\,\text{mm}^3$, and the isolation achieved in the lower band is 10 dB was not at all satisfactory. To get satisfactory isolation, orthogonal placement of two ports is considered in the design process as shown in Fig. 5(b), and the obtained isolation is satisfactory with overall dimensions $54 \times 25 \times 1.6\,\text{mm}^3$.

In this method, the achieved isolation is as low as 22 dB in the lower band. This improvement can be attributed to pattern diversity. For improving the channel capacity further, a four-port configuration is considered as shown in Fig. 5(c). Sufficient isolation is obtained in this case which is required for satisfactory MIMO performance. By using square geometry ($50 \times 50\,\text{mm}^2$), the shift in operating bands is nullified. The reason behind such a square dimension is to suppress the coupling between the fields of port-1 and port-2.

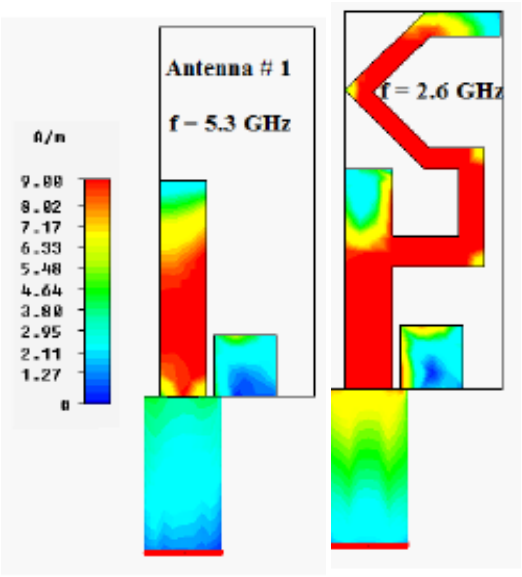

Figure 4. Surface current distribution characteristics of the ACS fed Hook shaped multiband antenna at 2.4 GHz, 5.5 GHz.

2.3. Configuration of Proposed MIMO Antenna

As shown in Fig. 6, the geometry of proposed Hook shaped ACS fed four-port MIMO antenna system is fabricated on an FR-4 substrate having dimensions of $50 \times 50 \times 1.6\,\text{mm}^3$, and the pattern diversity achieved by the orthogonal placement of antenna elements will help achieve the increased isolation between port 1 and port 2 fields. By placing the antenna elements very closely, the effective length of the antenna should be increased, which results in shifting of lower and higher operating bands. A shift in the higher band is comparatively negligible, and it covers the required band of operation. In order to compensate this shift, lengths of radiating paths corresponding to the lower and higher operating bands were reduced accordingly, and updated values are shown in Fig. 1.

3. RESULTS AND DISCUSSION

In this section, the simulated and measured results of the proposed 4-port MIMO antenna are discussed using the CST microwave studio suite. A coaxial cable of 50 ohms is used to feed the antenna elements. The prototype view of the four-port hook shaped MIMO antenna is shown in Fig. 7.

3.1. Scattering Parameters

S-parameters describe the response of an N-port network to signal(s) incidents to any or all of the ports. For a good antenna, reflection coefficient should be $< -10\,\text{dB}$, and the S-parameters of the proposed design are simulated using CST microwave studio software. The results of the proposed design show that return loss is $< -20\,\text{dB}$ in 2.25 GHz to 2.4 GHz (lower band) and $< -15\,\text{dB}$ in 4.7 GHz to 6.3 GHz (higher band). Fig. 8 shows the reflection coefficient at different frequencies including operating band frequencies. Orthogonal geometry is adopted for improving the isolation between the antenna elements. Mutual coupling coefficients (S_{12}, S_{13}, S_{14}) are less than $< -15\,\text{dB}$ that is within the acceptable level and are observed.

3.2. Radiation Patterns and Efficiency

A single port is excited using an SMA connector or coaxial cable of 50 ohms to feed the antenna elements, and the remaining ports are terminated by using a matched load for the single element radiation pattern.

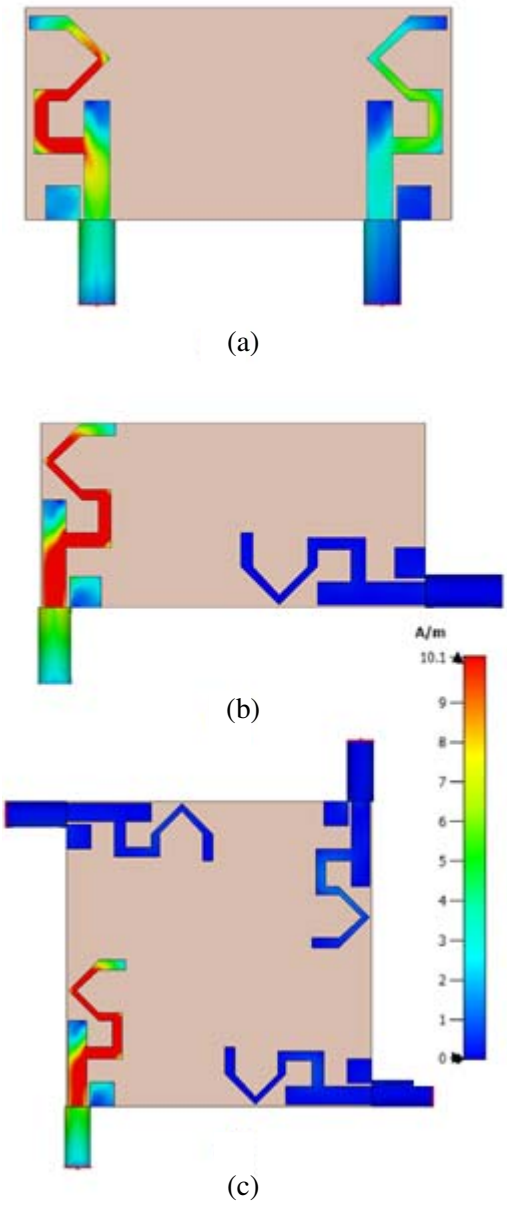

Figure 5. The surface current distribution in (a) parallel and (b) orthogonal configuration between two ports at 24 GHz, (c) surface current distribution of the proposed MIMO system in orthogonal configuration at 2.3 GHz.

The radiation pattern of the proposed MIMO antenna at different frequency bands is shown in Fig. 9. For better antenna performance, the efficiency should be as high as possible. The radiation efficiency is greater than 85% in the operating band which is shown in Fig. 10. The measured peak gain of the proposed MIMO antenna is 4 dBi which is observed at the operating band frequency, and Fig. 10 depicts simulated efficiency and measured gain against the frequency plot.

4. DIVERSITY PARAMETERS

We need to extract and analyse the diversity parameters of MIMO antenna such as Envelope Correlation Coefficient, Mean Effective Gain, Diversity Gain, Total Active Reflection Coefficient, and Channel Capacity Loss for understanding the advantages and also the performance of the MIMO system.

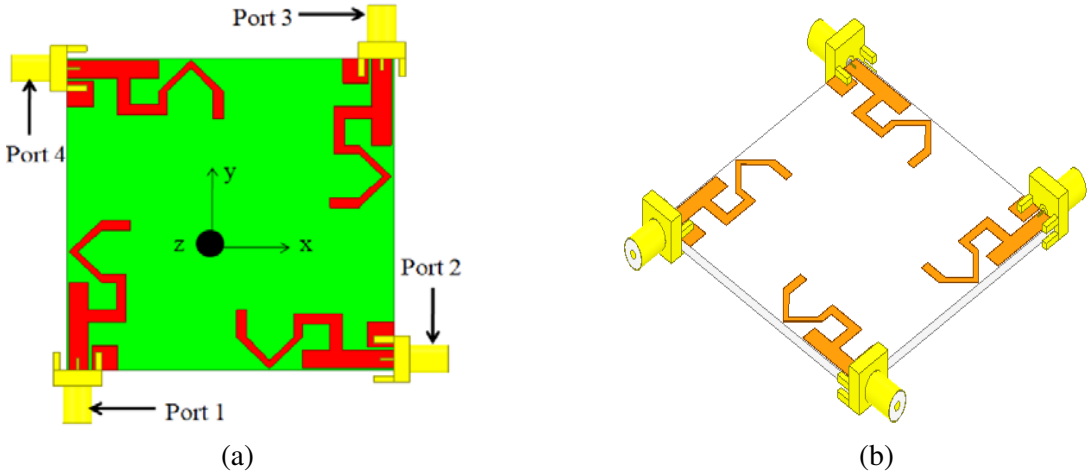

Figure 6. (a) Geometry of the proposed four-port Hook shaped MIMO antenna design. (b) 3-D view of proposed Hook shaped MIMO antenna.

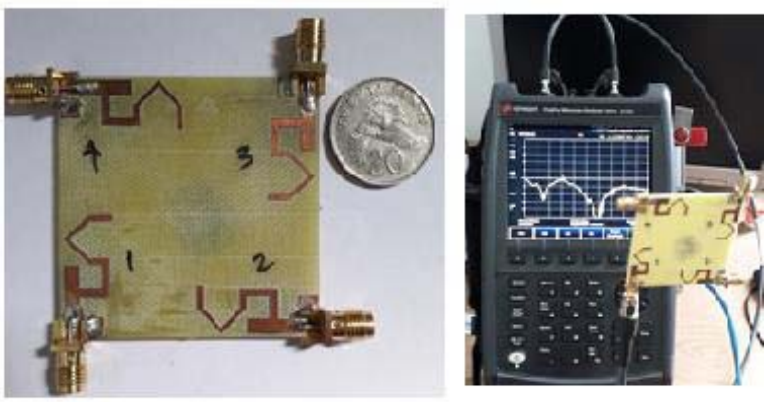

Figure 7. Prototype of Hook shaped MIMO antenna.

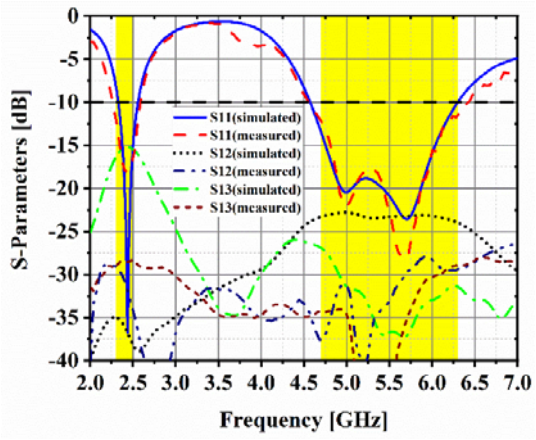

Figure 8. Reflection coefficient of proposed Hook shaped MIMO design.

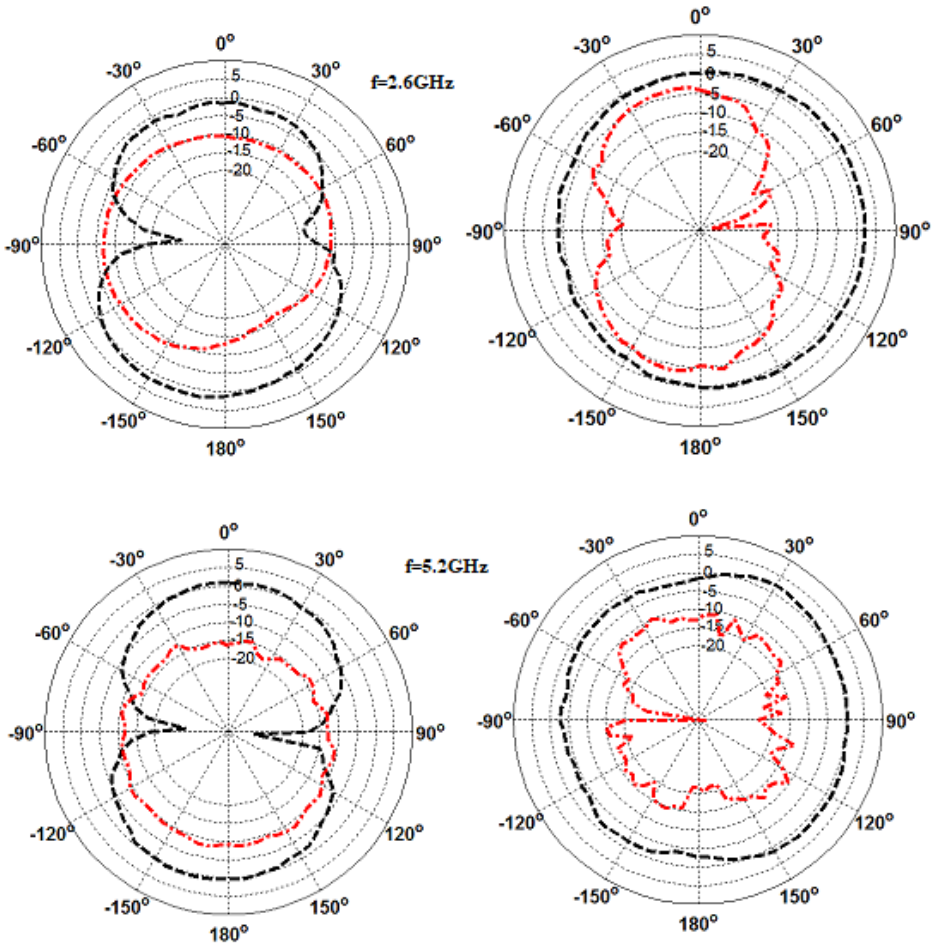

Figure 9. 2-D radiation patters of the proposed Hook shaped ACS fed MIMO antenna.

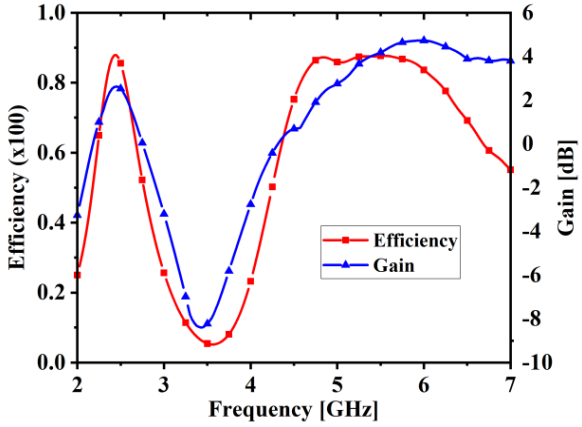

Figure 10. Total efficiency and gain of the proposed MIMO antenna.

4.1. ECC and DG

Generally, ECC is the pattern independence and diversity performance of antenna elements. For the high performance in the MIMO system, the ECC is a lower value between the antenna elements. When being operated concurrently, the ECC considers the effect of one radiation pattern over the other and

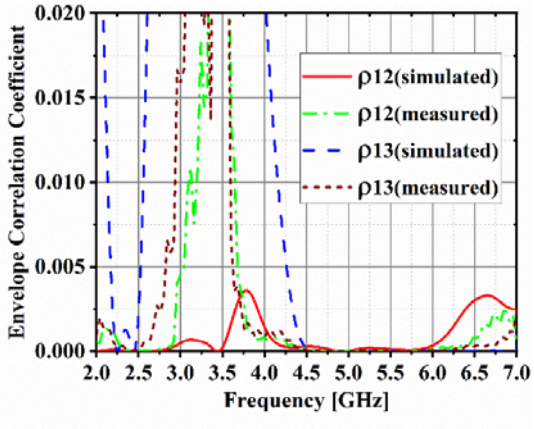

Figure 11. The envelope correlation coefficient of the proposed MIMO antennas.

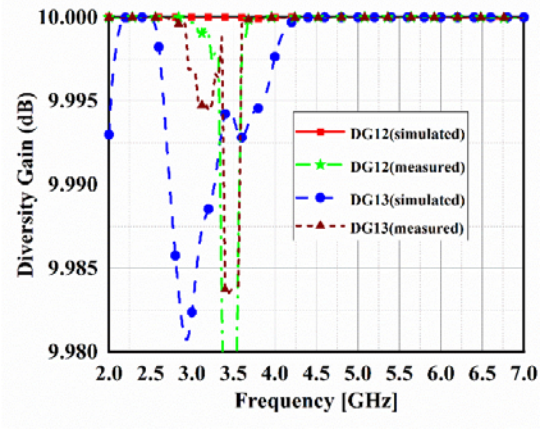

Figure 12. Diversity gain of proposed MIMO antenna.

can be calculated by Equation (1) which is observed in Fig. 11.

$$\mathrm{ECC} = \rho e = \left| \frac{\left| S_{ii}^{*} S_{ij} + S_{ji}^{*} S_{jj} \right|}{\left| \left(1 - |S_{ii}|^2 - |S_{ij}|^2\right) \left(1 - |S_{jj}|^2 - |S_{ji}|^2\right) \right|^{\frac{1}{2}}} \right|^2 \tag{1}$$

The diversity gain of the proposed antenna is observed in Fig. 12. Utilization of diverse radiating antenna elements presents with numerous channel paths to transmit, where multiple versions of the transmissions are acquired, and this effect can be evaluated by the diversity gain and evaluated in Equation (2).

$$\mathrm{DG} = 10 \times \sqrt{1 - |\mathrm{ECC}|^2} \tag{2}$$

From Figs. 11 & 12, it is clear that ECC should be less than 0.025, and DG should be greater than 9.95 that is within acceptable limits for the proposed four-port ACS fed hook shaped MIMO antenna.

4.2. Mean Effective Gain (MEG)

MEG is a prominent parameter in diversity analysis, and it is the ratio of the average power received by the antenna which is under test to the average power received by a reference antenna in the same environment. By using transmission coefficient characteristics, the MEG can be computed as below. The comprehensive difference between any two MEG waveforms should be less than 3 dB which is shown in Fig. 13.

$$\mathrm{MEG} = 0.5 \left[1 - \sum\nolimits_{j=1}^{N} |S_{ij}|^2 \right] \tag{3}$$

also

$$|\mathrm{MEG}_i - \mathrm{MEG}_j| < 3\,\mathrm{dB} \tag{4}$$

So, MEG can be written as

$$\mathrm{MEG1} = 0.5 \left[1 - |S_{11}|^2 - |S_{12}|^2 - |S_{13}|^2 - |S_{14}|^2 \right] \tag{5}$$

$$\mathrm{MEG2} = 0.5 \left[1 - |S_{21}|^2 - |S_{22}|^2 - |S_{23}|^2 - |S_{24}|^2 \right] \tag{6}$$

$$\mathrm{MEG3} = 0.5 \left[1 - |S_{31}|^2 - |S_{32}|^2 - |S_{33}|^2 - |S_{34}|^2 \right] \tag{7}$$

$$\mathrm{MEG4} = 0.5 \left[1 - |S_{41}|^2 - |S_{42}|^2 - |S_{43}|^2 - |S_{44}|^2 \right] \tag{8}$$

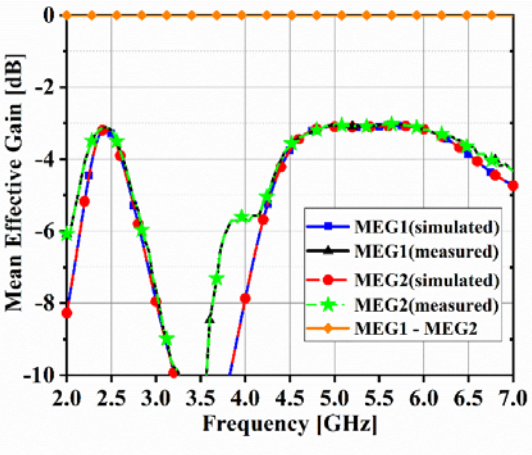

Figure 13. Mean effective gain of the proposed Hook shaped MIMO antenna.

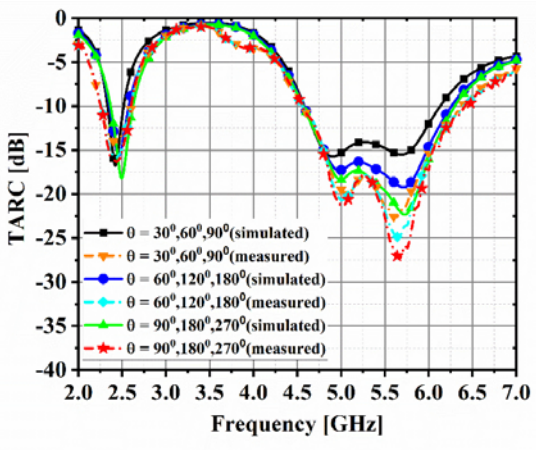

Figure 14. The total active radiation coefficient (TARC) of the proposed Hook shaped MIMO system vs frequency.

4.3. TARC

TARC can be defined as the ratio of the square root of total reflected power divided by the square root of total incident power. The system's response with respect to mutual coupling and the random signal combinations among the ports are thoroughly presented to us by TARC which can be calculated using Equation (9), and the simulated response is shown in Fig. 14.

$$\text{TARC} = \frac{\sqrt{\sum_{i=1}^{N}\left|S_{i1}+\sum_{m=2}^{N}S_{im}e^{j\theta_{m-1}}\right|^2}}{\sqrt{N}} \tag{9}$$

4.4. Channel Capacity Loss (CCL)

CCL is used to evaluate the performance of the MIMO system. The CCL increases with a linear relationship with increasing the number of antenna elements in any system without changing the bandwidth of transmitted power. The following Equation (10) can be used for computing CCL.

$$C_{\text{loss}} = -\log_2\det(\alpha^R) \tag{10}$$

$$\alpha^R = \begin{bmatrix} \alpha_{11} & \alpha_{12} & \alpha_{13} & \alpha_{14} \\ \alpha_{21} & \alpha_{22} & \alpha_{23} & \alpha_{24} \\ \alpha_{31} & \alpha_{32} & \alpha_{33} & \alpha_{34} \\ \alpha_{41} & \alpha_{42} & \alpha_{43} & \alpha_{44} \end{bmatrix} \alpha_{ii} = 1 - \left(\sum_{j=1}^{N}|S_{ij}|^2\right) \tag{11}$$

$$\alpha_{ij} = -\left(S_{ii}^{*}S_{ij} + S_{ji}^{*}S_{jj}\right) \tag{12}$$

The CCL for the proposed MIMO antenna is shown in Fig. 15. It shows that the measured and simulated results of the CCL are 0.2 bits/s/Hz where CCL value up to 0.4 bits/s/Hz is acceptable. Channel capacity of the proposed antenna is compared in Fig. 15(b) which is calculated using equations in [37]. A maximum channel capacity of 22.15 b/s/Hz is obtained when being measured whereas simulation-based value yields a maximum of 22.09 b/s/Hz.

5. INSTALLED ANTENNA RESULTS

To illustrate the potential of the proposed unit element for V2V communications, a full wave simulation using CST Studio Suite is performed to obtain both impedance matching and radiation characteristics.

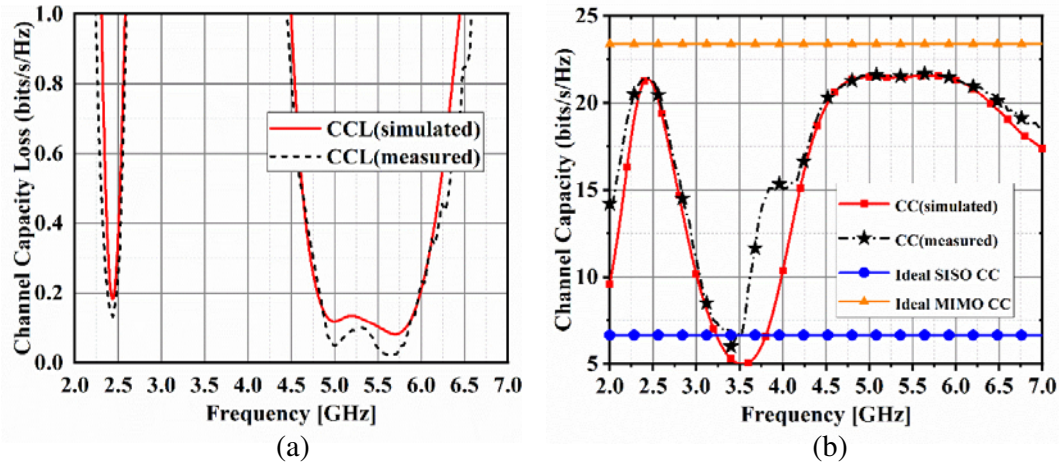

Figure 15. (a) CCL and (b) CC of the proposed 4 port Hook shaped MIMO antenna.

For simulation purpose, a sedan is used where the proposed unit element is mounted on its roof. Since this simulation involves a couple of billion mesh cells, radiation pattern at 5.9 GHz is only presented in Figs. 16(b) & (c). A maximum gain of 6.07 dB is obtained at 5.9 GHz while ensuring the omni-directionality for providing good coverage in vehicular environment. Many nulls in the pattern can be

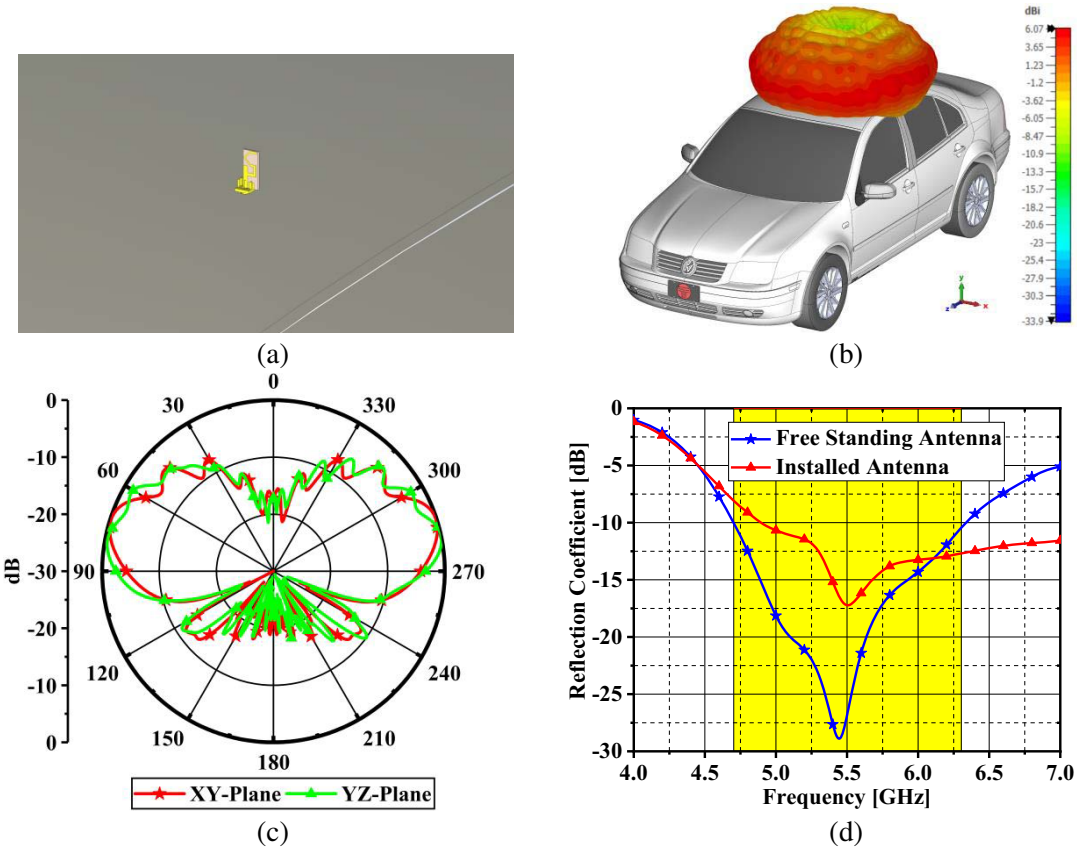

Figure 16. (a) Placement of antenna on roof of the car. (b) Installed 3D radiation pattern of the proposed antenna at 5.9 GHz. (c) Normalized radiation patterns at 5.9 GHz. (d) Comparison of $|S_{11}|$ in free standing and installed scenarios.

observed because antenna is backed by the metallic roof of the sedan. Due to the same reason, the magnitude of reflection coefficient of installed antenna (Fig. 16(d)) is deviated compared to what was obtained in the case of free-standing antenna. Despite the deviation, the installed antenna achieves a good $|S_{11}| < -13$ dB at 5.9 GHz. From all these results, the proposed antenna can be considered as a potential candidate for V2V applications.

6. CONCLUSION

This work presents a unique dual-band 4 element hook shaped MIMO antenna operating in the frequency bands of 2.25 to 2.4 and 4.7 to 6.3 GHz. The proposed antenna having a peak gain of 4 dB, and return loss is < -10 dB over dual bands. The orthogonal placement of antenna elements provides isolation of 16 dB with a radiation efficiency of 85%. The resulting envelope correlation coefficient, which is 0.025, is well below the standard limit (< 0.07) of wireless communication devices and thus making it suitable for WiBro, WLAN, and WiMAX applications. Simulated results for analysing the proposed antenna performance in installed scenario are presented to validate its potential use for V2V applications. The evaluated MEGs, diversity gain (DG), TARC, and CCL substantiate the MIMO performance of the antenna.

ACKNOWLEDGMENT

The authors would like to thank NPHSAT SYSTEMS PVT LTD (www.nphsat.com) for providing technical assistance for improving the manuscript and the authors thankfully acknowledges this publication as an outcome of the R&D work undertaken project (Project No: NPHSAT/R&D-02/2020-2022) NPHSAT SYSTEMS PVT LTD (www.nphsat.com), Vijayawada-520007, Andhra Pradesh, India.

REFERENCES

1. Xie, J. J., X. S. Ren, Y. Z. Yin, and S. L. Zuo, "Rhombic slot antenna design with a pair of straight strips and two ∩-shaped slots for WLAN/WiMAX applications," *Microwave and Optical Technology Letters*, Vol. 54, No. 6, 1466–1469, 2012.
2. Yoon, J. H. and G. S. Kil, "Compact monopole antenna with two strips and a rectangular-slit ground plane for dual-band WLAN/WiMAX applications," *Microwave and Optical Technology Letters*, Vol. 54, No. 7, 1559–1566, 2012.
3. Al-Khaldi, M., "A highly compact multiband antenna for Bluetooth/WLAN, WiMAX, and Wi-Fi applications," *Microwave and Optical Technology Letters*, Vol. 59, No. 1, 77–80, 2017.
4. Sun, X. L., L. Liu, S. W. Cheung, and T. I. Yuk, "Dual-band antenna with compact radiator for 2.4/5.2/5.8 GHz WLAN applications," *IEEE Transactions on Antennas and Propagation*, Vol. 60, No. 12, 5924–5931, 2012.
5. Hua, M., P. Wang, Y. Zheng, H. Qin, and W. Liu, "Compact dual-band CPW-fed antenna for WLAN applications," *2013 International Workshop on Microwave and Millimeter Wave Circuits and System Technology (MMWCST)*, 83–85, IEEE, October 2013.
6. Naidu, P. V., et al., "Design and development of triple band ACS fed antenna with M and rectangular shaped radiating branches for 2.45/5 GHz wireless applications," *Microsystem Technologies*, Vol. 23, No. 12, 5841–5848, 2017.
7. Kumar, A., et al., "A novel ACS fed multi band antenna loaded with mirrored S and L shaped strips for advanced portable wireless communication applications," *Microsystem Technologies*, Vol. 23, No. 10, 4775–4783, 2017.
8. Naidu, P. V., et al., "A small asymmetric coplanar strip fed tri-band antenna for PCS/WiMAX/WLAN applications," *Microsystem Technologies*, Vol. 23, No. 1, 13–22, 2017.
9. Kumar, A. and P. V. Naidu, "A compact O-shaped printed ACS fed monopole dual-band antenna for 2.4 GHz Bluetooth and 5 GHz WLAN/WiMAX applications," *2016 Progress In Electromagnetic Research Symposium (PIERS)*, 2004–2008, Shanghai, China, Aug. 8–11, 2016.

10. Kumar, A. and P. V. Naidu, "A novel compact printed ACS fed dual-band antenna for Bluetooth/WLAN/WiMAX applications," *2016 Progress In Electromagnetic Research Symposium (PIERS)*, 2000–2003, Shanghai, China, Aug. 8–11, 2016.
11. Kumar, R., P. Naidu, and V. Kamble, "Design of asymmetric slot antenna with meandered narrow rectangular slit for dual band applications," *Progress In Electromagnetics Research B*, Vol. 60, 111–123, 2014.
12. Naidu, P., et al., "A compact dual-band octagonal slotted printed monopole antenna for WLAN/WiMAX and UWB applications," *Journal of Microwaves, Optoelectronics and Electromagnetic Applications*, Vol. 14, No. 1, 1–13, 2015.
13. Naidu, P. and R. Kumar, "Design of CPW-fed dual-band printed monopole antennas for LTE/WiMAX/WLAN and UWB applications," *Progress In Electromagnetics Research C*, Vol. 54, 103–116, 2014.
14. Kumar, R., et al., "A compact asymmetric slot dual band antenna fed by CPW for PCS and UWB applications," *International Journal of RF and Microwave Computer-Aided Engineering*, Vol. 25, No. 3, 243–254, 2015.
15. Sun, D., et al., "A novel dual-band MIMO antenna with two rings for WIMAX applications," *Journal of Electromagnetic Waves and Applications*, Vol. 32, No. 3, 274–280, 2018.
16. Arun, M. S. and M. S. Parihar, "A frequency reconfigurable/switchable MIMO antenna for LTE and early 5G applications," *AEU-International Journal of Electronics and Communications*, Vol. 131, 153638, 2021.
17. Lee, W.-W. and Y.-S. Cho, "A high-isolation MIMO antenna with dual-feed structure for WiFi of mobile phones," *Microwave and Optical Technology Letters*, Vol. 59, No. 4, 930–934, 2017.
18. Mohammad-Ali-Nezhad, S. and H. R. Hassani, "A penta-band printed monopole antenna for MIMO applications," *Progress In Electromagnetics Research C*, Vol. 84, 241–254, 2018.
19. Khan, M. U. and M. S. Sharawi, "A dual-band microstrip annular slot-based mimo antenna system," *Microwave and Optical Technology Letters*, Vol. 57, No. 2, 360–364, 2015.
20. Birwal, A., et al., "Low-profile 2.4/5.8 GHz MIMO/diversity antenna for WLAN applications," *Journal of Electromagnetic Waves and Applications*, Vol. 34, No. 9, 1283–1299, 2020.
21. Cui, S., et al., "Compact dual-band monopole antennas with high port isolation," *Electronics Letters*, Vol. 47, No. 10, 579–580, 2011.
22. Ling, X. and R. L. Li, "A novel dual-band MIMO antenna array with low mutual coupling for portable wireless devices," *IEEE Antennas and Wireless Propagation Letters*, Vol. 10, 1039–1042, 2011.
23. Fang, Q., D. Mi, and Y.-Z. Yin, "A tri-band MIMO antenna for WLAN/WiMAX application," *Progress In Electromagnetics Research Letters*, Vol. 55, 75–80, 2015.
24. Addaci, R., et al., "Dual-band WLAN diversity antenna system with high port-to-port isolation," *IEEE Antennas and Wireless Propagation Letters*, Vol. 11, 244–247, 2012.
25. Ali, W. A. E., M. I. Ashraf, and M. A. Salamin, "A dual-mode double-sided 4×4 MIMO slot antenna with distinct isolation for WLAN/WiMAX applications," *Microsystem Technologies*, Vol. 27, No. 3, 967–983, 2021.
26. Fang, H.-S., et al., "Design of a compact MIMO antenna with pattern diversity for WLAN application," *Microwave and Optical Technology Letters*, Vol. 59, No. 7, 1692–1697, 2017.
27. Huang, J., et al., "A quad-port dual-band MIMO antenna array for 5G smartphone applications," *Electronics*, Vol. 10, No. 5, 542, 2021.
28. Deng, J. Y., et al., "A dual-band MIMO antenna decoupled by a meandering line resonator for WLAN applications," *Microwave and Optical Technology Letters*, Vol. 60, No. 3, 759–765, 2018.
29. Zou, X. J., et al., "Decoupling of dual-band closely spaced MIMO antennas based on novel coupled resonator structure," *Frequenz*, Vol. 72, Nos. 9–10, 437–441, 2018.
30. Liu, Y., et al., "A novel four-port high isolation MIMO antenna design for high-capacity wireless applications," *Microwave and Optical Technology Letters*, Vol. 60, No. 6, 1476–1481, 2018.

31. See, C. H., et al., "Wideband printed MIMO/diversity monopole antenna for WiFi/WiMAX applications," *IEEE Transactions on Antennas and Propagation*, Vol. 60, No. 4, 2028–2035, 2012.
32. Ghosh, C. K., "A compact 4-channel microstrip MIMO antenna with reduced mutual coupling," *AEU International Journal of Electronics and Communications*, Vol. 70, No. 7, 873–879, 2016.
33. Malviya, L., M. V. Kartikeyan, and R. K. Panigrahi, "Offset planar MIMO antenna for omnidirectional radiation patterns," *International Journal of RF and Microwave Computer-Aided Engineering*, Vol. 28, No. 6, e21274, 2018.
34. Huang, H., Y. Liu, and S.-X. Gong, "Four antenna MIMO system with compact radiator for mobile terminals," *Microwave and Optical Technology Letters*, Vol. 57, No. 6, 1281–1286, 2015.
35. Kumar, A., et al., "An ultra-compact two-port UWB-MIMO antenna with dual band-notched characteristics," *AEU-International Journal of Electronics and Communications*, Vol. 114, 152997, 2020.
36. Kumar, A., P. Naidu, V. Kumar, and A. K. Ramasamy, "Design & development of compact uniplanar semi-hexagonal ACS fed multi-band antenna for portable system application," *Progress In Electromagnetics Research M*, Vol. 60, 157–167, 2017.
37. Sharawi, M. S., *Printed MIMO Antenna Engineering*, Artech House, 2014.